



DEFORMATION MONITORING AT AN INDUSTRIAL SITE USING COMBINED DGPS AND TOTAL STATION DATA

Axel Ebeling¹, Robert Radovanovic² and Bill Teskey¹

¹ *Department of Geomatics Engineering, Schulich School of Engineering,
University of Calgary, Calgary, Alberta, CANADA*

² *Principal, SARPI Ltd., Edmonton, Alberta, CANADA*

Abstract: A large deformation monitoring network has been observed in three epochs. Heterogeneous data were collected on two unstable slopes near a cooling water pond for a power generation plant. These heterogeneous data consist of horizontal directions, horizontal distances and trigonometric height differences derived from total station observations and azimuths, distances and ellipsoidal height differences derived from DGPS observations. A separate network adjustment is performed for each epoch to integrate the heterogeneous data and obtain coordinates of all stations in a local level frame. Then, a Multi-Parameter Transformation is applied to compare coordinates between epochs. In the MPT method, a three-dimensional similarity transformation (three rotations, three translations, and a scale factor) is used to relate observations or derived observations (e.g. coordinates) from different measurement epochs. A global best fit will yield three-dimensional differences of all stations between measurement epochs. Statistical verification of these differences allows to distinguish between apparent movements due to random observation errors and actual deformations. Furthermore, a priori knowledge of the unknown transformation parameters can be utilized to strengthen the solution. Results from this application indicate that a Multi-Parameter Transformation is a very effective method for deformation monitoring, especially when a large number of the monitored points show significant deformations.

1. INTRODUCTION

A large deformation monitoring network has been observed in three epochs between 2005 and 2007. The network is spread out over two unstable slopes (North Hill and Rom Hill) near a cooling water pond for a large coal-fired electric power generation plant. There are no stable control stations in the area, all network points are potentially subject to deformations. Heterogeneous data derived from Total Station and GPS measurements are available for all three epochs.



The goal is to determine significant movements of the two hill sides over time from the given observations. Section 2 introduces the monitoring network and describes the measurements carried out and their accuracies.

In the first step of the analysis, a separate network adjustment is performed for each epoch to integrate the heterogeneous data and obtain local coordinates of all points. This is described in section 3.

In the second step, a Multi-Parameter Transformation is applied to compare coordinates between epochs and obtain misclosure vectors for all points. These misclosure vectors are then statistically verified to distinguish between apparent movements due to random measurement errors and actual deformations of the target points. This deformation analysis is described in section 4.

Section 5 presents results obtained from the analysis described previously, which are deformations of the two hill sides between the 2005 and 2006 measurement campaign as well as between the 2005 and 2007 epochs. A discussion of these results follows.

Lastly, section 6 summarizes this paper and offers conclusions derived from the results obtained in the analysis.

2. NETWORK AND OBSERVATIONS

The monitoring network consists of 55 points in total, although not all points were observed in each epoch. The points are located on two separate hill sides (North Hill and Rom Hill) near a water reservoir for a power generation plant. North Hill (Figure 1a) is facing the reservoir on the North side. Rom Hill (Figure 1b) is located just south of the plant itself. Figure 2 gives an overview of the point locations. Points 11 to 29 and 110 to 114, marked in blue, are on North Hill. Points 31 to 39 and 311 to 319, marked in brown, are located on Rom Hill. Points 41 to 48 (green) are piezometer locations on North Hill. Points 400 to 406 (gray) are temporary points. Points 402 and 405 are located in the valley between the two hill sides.



Figure 1a - North Hill



Figure 1b - Rom Hill

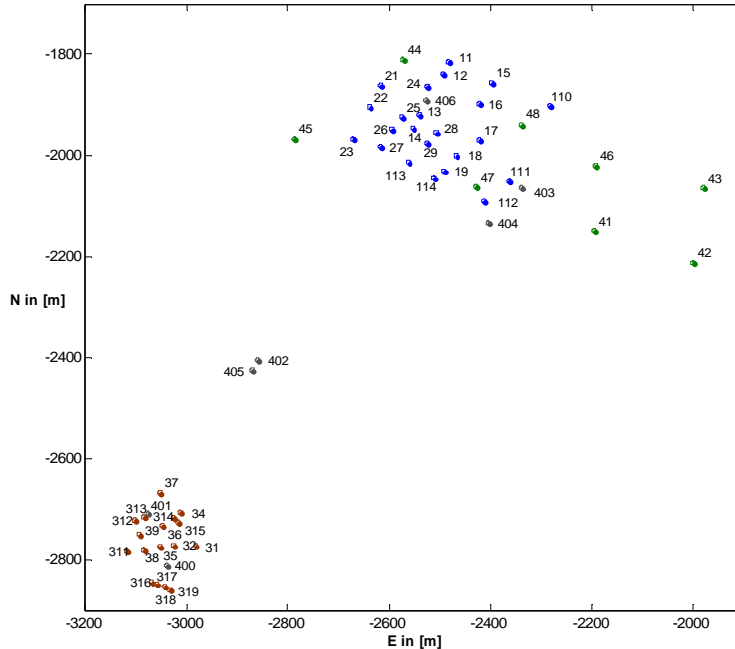


Figure 2 - Location of Target Points

Accuracies for Total Station measurements are given with 5 arc seconds for horizontal directions and zenith angles and 5mm for slope distances. On the GPS side, the accuracy for the pseudo-observation vectors are 5mm for Northing and Easting components and 15mm for heights. All observations are assumed to be uncorrelated. By applying the law of propagation of errors, accuracies for the observations described above can be estimated.

3. INTEGRATION OF HOMOGENEOUS DATA

When integrating GPS-derived and terrestrial observations a number of things have to be considered. First of all, terrestrial distances are given with respect to the local horizontal plane of the instrument station and not with respect to the mapping surface of the GPS observations. Therefore, a scale factor has to be introduced to map horizontal distances from Total Station measurements to the reference surface specified by GPS.

Another fact that has to be considered is the difference between orthometric heights as obtained from terrestrial observations and ellipsoidal heights from GPS. The difference between the two at a certain point is the geoid undulation N , (Seeber, 2003). Since in this case only height *differences* between points are available, only the *change* in geoid undulation ΔN between points is of interest. The power generation plant where the observations were collected is located in the prairies on relatively flat terrain. Also is the area under consideration comparatively small (about 1.5 km²). For these reasons, the geoid undulation can be assumed to be constant. Conclusively, changes in geoid undulation across the area will



be zero and terrestrial and ellipsoidal height differences can be considered equal within the given accuracy of the observations.

The first step of the analysis consists of a separate network adjustment of each epoch. This is done to integrate the different kinds of observations available and thus obtain “homogeneous” coordinates for all points in a uniform coordinate system. Their standard deviations can also be estimated, which are crucial for the subsequent deformation analysis. Furthermore, the network adjustment allows to detect and eliminate outliers in the observations and to gain an insight in the reliability of the data.

Another important aspect is the definition of the geodetic datum of the network. Since this is a 3D network, there are seven datum parameters to be determined: three translations along the coordinate axes, three rotations about the coordinate axes and a scale factor.

However, some of these parameters are already defined by the observations themselves. The scale factor is given by the distances on the mapping surface derived from GPS data. Rotations around the two horizontal axes are fixed since observations have been carried out with respect to a local horizontal plane. The rotation about the vertical axis is defined by the azimuth observations available from GPS. Thus, only three free parameters remain, the three translations along the coordinate axes.

There are a number of ways to overcome this datum defect. However, since this is a deformation monitoring network, it is important that the inner geometry of the network is not distorted by the datum points. So an over-constrained approach should be avoided.

Traditionally, a deformation monitoring network consists of a number of control stations which are located on stable ground and target points attached to the observed object. The first group is used to define the datum, the latter represents the movement of the monitored structure, (Möser et al., 2000). In the application at hands this is not the case. There are no control stations available that can be considered as stable. The network consists solely of target points that are potentially subject to deformations.

For this reason, the employed strategy is to use all available points and apply inner constraints to define the geodetic datum of the network. In this approach, the coordinate changes applied to the estimates are minimized and the inner geometry of the network is not affected.

Once the datum definition is clear, coordinates for all points and fully populated covariance matrices can be obtained by performing a parametric, non-linear least-squares adjustment. The observation equations are given by the relations between the observations and the unknown coordinates. Initial estimates for the unknown coordinates are available.

In the case at hands, inner constraints have been applied to points *common to all three* measurement epochs (48 points), to define the three translations of the geodetic datum. Thus, all three epoch share the same datum.

4. DEFORMATION ANALYSIS

To obtain deformations from the adjusted coordinates of each epoch, a Multi-Parameter-Transformation is applied. The 2005 epoch serves as original (reference) epoch while the data



from 2006 and 2007 respectively, are considered as repeated epochs. As a result, movements between 2005 and 2006 as well as movements between 2005 and 2007 will be derived.

A Multi-Parameter-Transformation is essentially a seven parameter similarity transformation between the original and repeated epoch, (Teskey et al., 2006). It is a very flexible solution since it can utilize different data as input, e.g. Total Station observations (horizontal circle readings, vertical circle readings and slope distances) or DGPS baselines. In this application, the MPT method is for the first time directly applied to coordinates of a complete, large-scale deformation monitoring network with virtually no stable control stations available.

The Multi-Parameter-Transformation relates observations from the original epoch $\overset{w}{X}_O$ to those of the repeated epoch $\overset{w}{X}_R$ by applying a rotation, translation and a scale factor between epochs, (Teskey et al., 2006). This can be expressed as:

$$\overset{w}{X}_O = \lambda \cdot (\mathcal{Q} \overset{w}{X}_R \cdot \mathcal{Q}^{-1}) + \overset{w}{T} \quad (1)$$

where $\overset{w}{T} = (T_x, T_y, T_z)^T$ denotes the translation parameters and λ is the change in scale between epochs. In the case at hands, observations of the original epoch are the adjusted coordinates of the 2005 epoch and observations of the repeated epoch are the adjusted coordinates of the 2006 and 2007 epochs respectively. They can be expressed as:

$$\overset{w}{X}_O = \begin{pmatrix} N \\ E \\ h \end{pmatrix}_O \quad \overset{w}{X}_R = \begin{pmatrix} N \\ E \\ h \end{pmatrix}_R \quad (2)$$

Note that a quaternion approach has been chosen in (1) to represent the rotation between epochs. Quaternions are essentially an expansion of complex numbers with one real part (q_0) and three imaginary (q_x, q_y, q_z) and can be written as $\mathcal{Q} = [q_0, (q_x, q_y, q_z)]$. They represent a rotation in 3D space as a single rotation with the rotation angel θ around a unit vector $(r_x, r_y, r_z)^T$ where

$$\begin{aligned} q_0 &= \cos\left(\frac{\theta}{2}\right) \\ q_x &= r_x \cdot \sin\left(\frac{\theta}{2}\right) \\ q_y &= r_y \cdot \sin\left(\frac{\theta}{2}\right) \\ q_z &= r_z \cdot \sin\left(\frac{\theta}{2}\right) \end{aligned} \quad (3)$$

The advantage of quaternions over Euler angles is that no trigonometric functions have to be applied to describe the rotation, which yields a bi-linear, numerically more stable normal equation system.



Furthermore, no initial estimates for the quaternion have to be computed, which is critical when using elementary rotations (ω , φ , κ) to converge to the correct solution. Any arbitrary values can be chosen as initial estimates for the components of the quaternion as long as the constraint

$$\|q\| = \sqrt{q_0^2 + q_x^2 + q_y^2 + q_z^2} = 1 \quad (4)$$

is fulfilled. For more information on quaternions, refer to (Kuipers, 2002).

By inserting equation (2) into equation (1), one obtains three linearly independent equations for each point observed in both, original and repeated epoch. The coordinates in each epoch are known, but the transformation parameters are not. If three or more common points were observed in each epoch, an overdetermined problem exists which can be solved in an implicit, bi-linear least-squares adjustment.

A further advantage of a Multi-Parameter-Transformation is that it allows to incorporate a priori knowledge of the unknown transformation parameters in the solution. This information can be introduced as additional observations, which increases redundancy and is especially helpful if a large number of points are suspected to have moved.

Results of the Multi-Parameter-Transformations are the adjusted transformation parameters and more importantly a misclosure vector for each point and its corresponding covariance matrix. From the latter, a strict statistical test can be performed in order to determine whether or not the computed misclosure is significant, i.e. if real deformations are inherent or just random observation errors.

In the case at hands, the 2005 epoch serves as reference. As all three measurement epochs are in the same datum, the translations and rotations between epochs are zero and the scale factor is one. Since all points have to be considered as potentially unstable, it is important to fix these transformation parameters between epochs as tightly as possible, i.e. to introduce the (a priori known) transformation parameters as observations and assign them a high weight.

This is done to assure the correct detection of movements. The transformation will yield a global best fit for all points in the two epochs. If no stable computational base is available and transformation parameters are determined from unstable points, these parameters will have a smoothing effect on the computed movements. They can be seen as some kind of average movement of all points and the movements obtained will merely show a deviation from that.

5. RESULTS

As a result from the Multi-Parameter-Transformation, 3D-movements and their standard deviations are available for all points. These standard deviations are then used to distinguish between apparent movements due to random errors in the observations and real deformations.



It has been found that the detectability for horizontal movements is at the 1 cm level while for the vertical component the detectability is about 2 cm.

Following is a table of the movements on North Hill for the epochs 2005 / 2006 and 2005 / 2007, respectively. Given are the movements with respect to North, East and height as well as the total 3D movement Δ . Points showing statistically significant deformations are highlighted.

It is obvious that between 2005 and 2007 most of the points on North Hill show significant deformations. These movements occur mainly in the horizontal while there are, with a few exceptions, no vertical movements apparent. The general direction of the horizontal movements is south-west, i.e. down-slope. The magnitude between 2005 and 2006 varies between 1 cm and 3 cm. In 2007, these movements have accumulated to up to 6 cm. The stable points are mainly piezometer locations. The following plot visualizes the North Hill movements where stable points are shown in blue while significant deformations are given in red.

2005 to 2006					2005 to 2007				
Point	N [m]	E [m]	H [m]	Δ [m]	Point	N [m]	E [m]	H [m]	Δ [m]
11	-0.016	0.018	0.004	0.025	11	-0.025	-0.013	-0.014	0.032
12	0.002	-0.014	0.013	0.019	12	-0.047	-0.024	0.016	0.055
13	-0.015	-0.005	0.002	0.015	13	-0.047	-0.022	0.007	0.052
14	-0.004	-0.005	0.001	0.007	14	-0.053	-0.024	0.014	0.059
15	0.007	0.000	-0.011	0.013	15	0.006	0.000	-0.004	0.007
17	0.007	-0.010	0.014	0.018	17	-0.048	-0.004	0.027	0.055
18	-0.005	-0.002	0.011	0.012	18	-0.064	-0.006	0.021	0.068
19	-0.002	-0.017	0.016	0.024	19	-0.003	-0.001	0.029	0.030
21	-0.016	0.006	-0.001	0.017	21	-0.045	-0.018	0.015	0.051
22	-0.004	0.004	0.002	0.006	22	-0.039	-0.021	0.019	0.048
23	-0.005	0.011	0.006	0.013	23	-0.012	-0.003	0.020	0.023
24	-0.004	0.005	-0.001	0.006	24	-0.054	-0.016	0.017	0.059
25	0.005	0.001	0.000	0.005	25	-0.050	-0.028	0.011	0.059
26	0.002	0.002	0.001	0.003	26	-0.034	-0.009	0.008	0.036
28	-0.014	-0.011	0.009	0.020	28	-0.056	-0.021	0.019	0.063
41	-0.001	-0.005	-0.012	0.013	41	-0.007	-0.006	-0.016	0.018
42	-0.002	0.007	0.010	0.012	42	0.005	0.011	0.006	0.013
43	0.007	0.001	-0.005	0.009	43	-0.006	-0.002	-0.009	0.011
44	-0.011	-0.007	0.000	0.013	44	-0.049	-0.029	0.004	0.057
45	0.013	0.004	-0.012	0.018	45	0.005	-0.002	-0.004	0.006
46	0.002	0.000	-0.002	0.003	46	-0.009	-0.006	-0.006	0.012
47	-0.004	0.004	-0.002	0.006	47	0.003	0.008	-0.018	0.020
48	0.003	0.002	0.011	0.012	48	-0.006	0.001	0.000	0.006
111	0.020	0.002	0.027	0.034	111	0.017	0.008	0.044	0.047
112	0.006	-0.006	0.015	0.017	112	-0.011	-0.015	0.021	0.028
113	0.013	0.003	0.001	0.014	113	-0.004	0.001	0.013	0.014
114	0.007	-0.003	0.018	0.019	114	-0.004	0.007	0.019	0.021

Table 1- Movements on North Hill

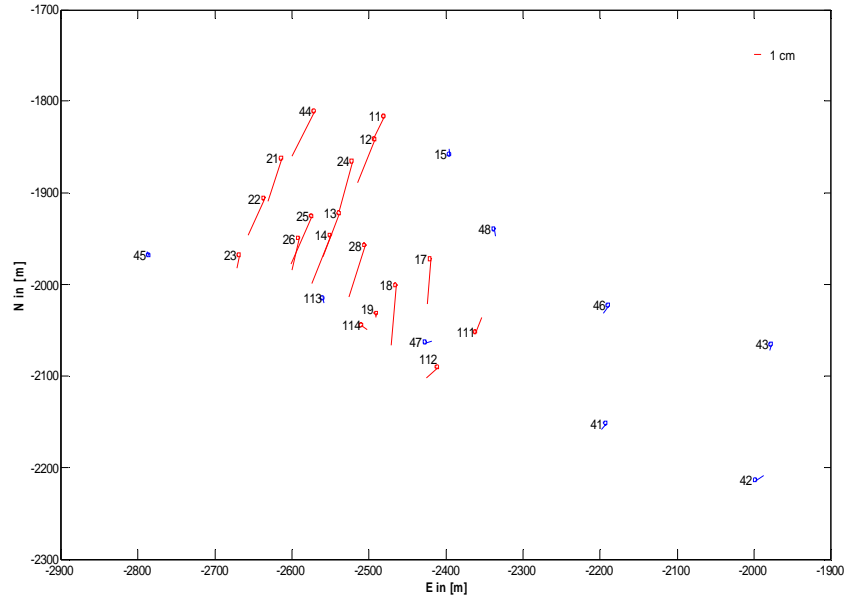


Figure 3 - Movements on North Hill

The following table shows the deformations of the points located on Rom Hill. Again, movements are given with respect to North, East, height as well as the total 3D-movement Δ . Points showing significant deformations are highlighted.

2005 to 2006				
Point	N [m]	E [m]	H [m]	Δ [m]
31	0.007	0.003	-0.056	0.056
32	0.006	-0.005	-0.052	0.052
34	0.003	-0.011	-0.049	0.051
35	0.011	-0.001	-0.049	0.050
36	-0.002	0.002	-0.051	0.051
37	0.007	0.007	-0.050	0.051
38	0.001	-0.004	-0.050	0.050
311	0.008	0.003	-0.044	0.045
312	0.008	0.005	-0.046	0.047
313	0.006	0.004	-0.048	0.049
314	0.009	-0.001	-0.044	0.045
315	0.008	0.005	-0.045	0.046
316	-0.007	0.003	-0.047	0.048
317	-0.009	0.004	-0.046	0.047
318	-0.003	0.007	-0.049	0.049
319	0.009	0.003	-0.043	0.044

2005 to 2007				
Point	N [m]	E [m]	H [m]	Δ [m]
31	0.009	0.002	-0.057	0.058
32	0.011	0.001	-0.047	0.048
34	0.006	-0.003	-0.052	0.053
35	0.013	-0.002	-0.045	0.047
36	-0.001	-0.008	-0.050	0.050
37	0.019	-0.002	-0.045	0.049
38	0.005	-0.003	-0.050	0.050
311	0.006	0.003	-0.049	0.049
312	0.010	-0.003	-0.046	0.047
313	0.007	0.000	-0.046	0.046
314	0.012	-0.004	-0.042	0.044
315	0.012	0.005	-0.044	0.046
316	0.001	-0.001	-0.043	0.043
317	0.001	0.002	-0.043	0.043
318	0.005	0.002	-0.044	0.044
319	0.009	0.005	-0.036	0.037

Table 2- Movements on Rom Hill

The 3D-plot below graphically shows the deformations of the Rom Hill points.

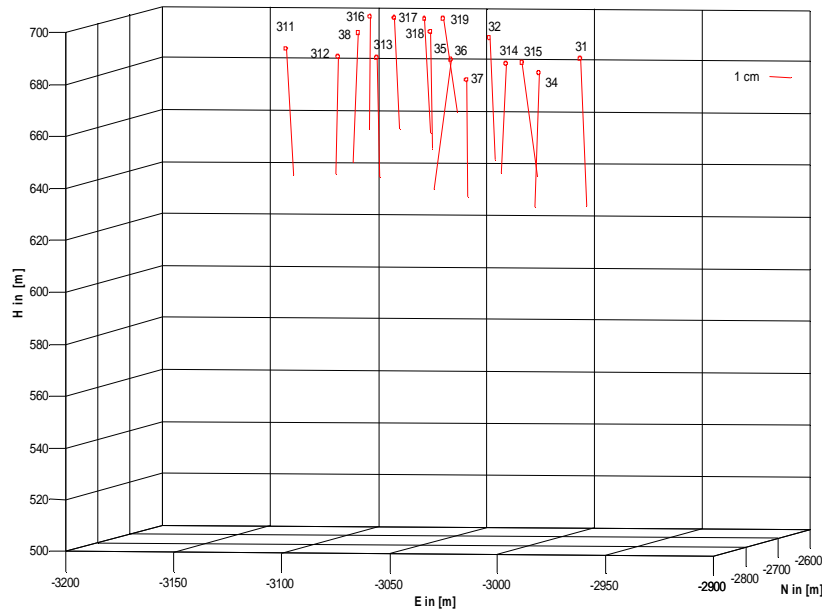


Figure 4 - Movements on Rom Hill

All points on Rom Hill show significant deformations. Unlike on North Hill, these deformations occur almost exclusively in vertical direction. These downward movements have magnitudes between 4.3 cm and 5.6 cm between 2005 and 2006 and remain stable since. This is interesting, since this significant downward movement is not accompanied by any horizontal component as would be expected on a moving slope. This and the fact that no further movements occurred after 2006 leads to the assumption that the slope itself is stable, but the bars constituting the points have settled by as much as 5 cm after the reference epoch was observed.

6. SUMMERY AND CONCLUSION

An industrial application for deformation monitoring has been introduced. By integrating the homogeneous data types available from three measurement epochs carried out between 2005 and 2007, coordinates for all target points can be derived. A Multi-Parameter-Transformation is then successfully applied to the whole monitoring network. Deformations could be recovered although no stable computational base is available. This is only possible by fixing the transformation parameters between epochs.

Results obtained for North Hill indicate a systematic, horizontal movement of about 5 cm in a downhill direction which is consistent with strong evidence of erosion on the hill. On Rom Hill a suspicious downward movement of all target points was detected between 2005 and



2006. This rather seems to be a movement of the target points themselves than a deformation of the hill. Further observation campaigns are needed to clarify this situation.

Conclusively, a Multi-Parameter-Transformation is a very suitable method for such applications. It allows to use data from different sources and yields 3D misclosure vectors with corresponding covariance information for each point observed in original and repeated epoch. It also has been shown that it works very reliably with a large number of unstable points which can be a crucial factor in a number of industrial applications or generally in areas where no stable reference is available.

References

- Kuipers, J. B. (2002). *Quaternions and Rotation Sequences: A Primer with Applications to Orbits, Aerospace and Virtual Reality*. Princeton and Oxford: Princeton University Press.
- Möser, M., Müller G., Schlemmer H., Werner H. (2000). *Handbuch Ingenieurgeodäsie: Auswertung geodätischer Überwachungsmessungen*. Heidelberg: Herbert Wichmann Verlag.
- Seeber, G. (2003). *Satellite Geodesy*. Berlin, New York: Walter de Gruyter.
- Teskey, W. F., Paul, B., Lovse, J. W. (2006). *Application of a Multi-Parameter-Transformation for Deformation Monitoring of a Large Structure*. Baden: Proceedings of the 12th International FIG Symposium on Deformation Measurements.

Corresponding author contacts

Axel Ebeling
aebeling@ucalgary.ca
Department of Geomatics Engineering, Schulich School of Engineering
University of Calgary, Calgary, Alberta
CANADA